Surface Crack Growth Under Three Point Bend And Tension Conditions

V.N. Shlyannikov, A.V.Tumanov

Research Center for Power Engineering Problems
Russian Academy of Sciences, 420111, Kazan, Lobachevsky Street, 2/31, Post/box 190
Tel/fax. +7(843) 258-13-05, +7(843) 236-31-02
e-mail: shlyannikov@mail.ru, tymanoff@rambler.ru

Keywords: semi-elliptical crack, crack growth resistance, strain-energy density, mixed mode, crack growth direction

1. Introduction

Surface flaws are typical damage to different types of engineering structures. The assessment of changes in both the form and the growth direction of the surface cracks during propagation is an essential element for the prediction of the structural integrity of biaxial loaded engineering structures such as pressured vessels, plane covering and pipelines in the presence of initial and accumulated operation damages. Literature review shows [1, 2] that the order of surface crack resistance characteristics determination is not full. Relationships between crack opening displacement and surface crack size are not provided. Moreover, surface cracks under mixed mode loading are not regulated by normative documents that is caused by mathematical and experimental methods complexity. Purpose of this work is an experimental substantiation of the developed criterion for surface cracks growth direction prediction under mixed mode loading and mode I surface crack resistance characteristics determination.

2. Inclined surface cracks stress-strain state

Is necessary to consider biaxiality, crack orientation angle, form and section position along curvilinear front for the inclined surface cracks (Fig.1) behavior description.

Load vector applied to remote plate surface is divided to three parts. Each vector corresponds to modes I, II and III and can be written as

$$\sigma_I^{\infty} = \frac{\sigma_{yy}^n}{2}\left(1+\eta-(1-\eta)\cos 2\alpha\right), \quad \sigma_{II}^{\infty} = \sigma_{yy}^n \frac{1-\eta}{2}\sin 2\alpha \cdot \cos\varphi,$$

$$\sigma_{III}^{\infty} = \sigma_{yy}^n \frac{1-\eta}{4}\sin 2\alpha \cdot \sin\varphi. \qquad (1)$$

where $\eta = \sigma_{xx}^n / \sigma_{yy}^n$ - biaxial ratio, $\sigma_{xx}^n, \sigma_{yy}^n$ - nominal stress applied to free surface, α - crack orientation angle, φ - position along curvilinear front (Fig.2).

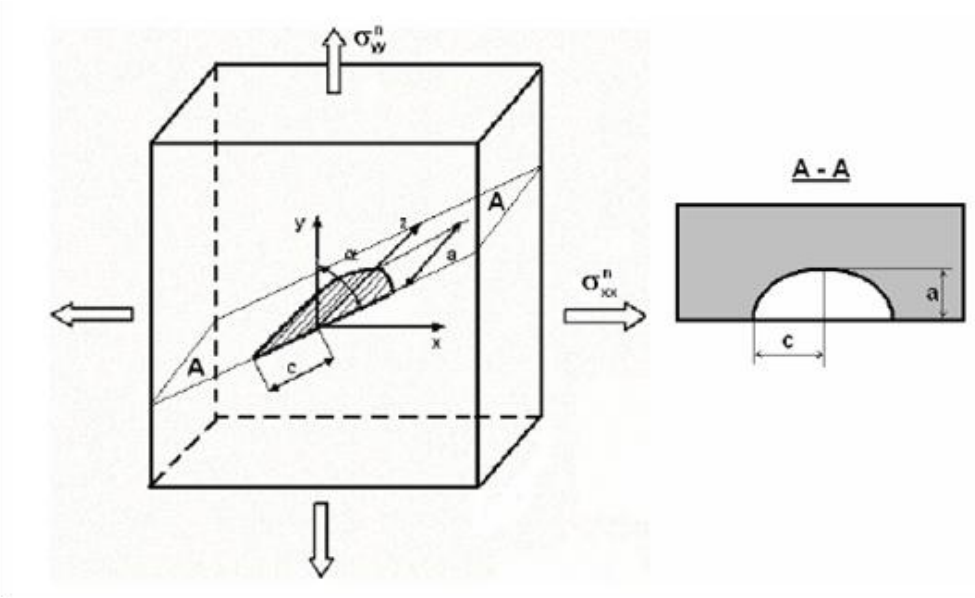

Figure 1. A semi-elliptical inclined surface crack in a plate under remote uniform biaxial loading

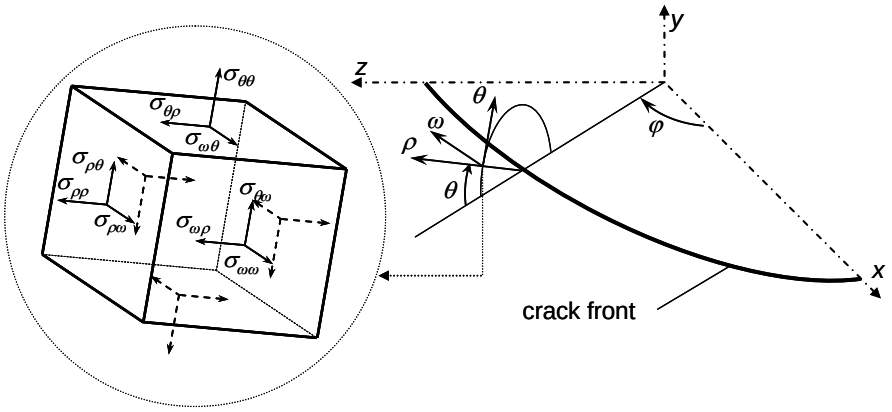

Figure 2. Used coordinate system

In general case modes I, II, III and stress intensity factors KI, KII, KIII are regarded as functions of the section position along curvilinear crack front. Based on computed three-dimensional finite element stress intensity factors, numerical results give one grounds for taking border effects for surface cracks into account. As a particular case of the mode II and mode III stress intensity factors the solution is proposed by He and Hutchinson [3] for arbitrary uniform remote stressing by the superposition of the stress intensity factors of the semi-elliptical surface crack as the sum of the reference intensity factors for the full elliptical crack with corrections by polynomials accounting for behavior in the vicinity of the corner. A useful reference solution concerns similarly aligned and loaded elliptical crack on an infinite solid. Analytical work by Kassir and Sih [4] analyzed the behavior of such an inclined, penny-shaped crack in an infinite medium under different uniform remote loading conditions. After taking load biaxiality into account and after using existing results for the mode I stress intensity factors [5], a general solution for the stress intensity factors can be written as the sum of the reference intensity factors for the full elliptical crack (the analytical solutions) with corrections by polynomials accounting for behavior in the vicinity of the corner (the FEA calculations)

$$K_I = \frac{K_I}{\sigma_I \sqrt{\pi l}} = K_I^{REF}\left[1+\eta-(1-\eta)\cos 2\alpha\right], \qquad K_{II} = \frac{K_{II}}{\sigma_{II}\sqrt{\pi l}} = K_{II}^{REF} + \delta_{II} K_{II}^{REF}\big|_{\max},$$

$$K_{III} = \frac{K_{III}}{\sigma_{III}\sqrt{\pi l}} = K_{III}^{REF} + 2\delta_{III} K_{III}^{REF}\big|_{\max}, \qquad (2)$$

Where,

$$K_I^{REF} = \frac{1}{2E_s} fF, \qquad K_{II}^{REF} = \frac{K_{II}}{\sigma_{II}\sqrt{\pi l}} = \frac{k^2 \varepsilon \cos\varphi}{2Bf}(1-\eta)\sin 2\alpha;$$

$$K_{III}^{REF} = \frac{K_{III}}{\sigma_{III}\sqrt{\pi l}} = \frac{k^2(1-\nu)\sin\varphi}{4Bf}(1-\eta)\sin 2\alpha. \qquad (3)$$

$$l = \frac{a}{\sqrt{\varepsilon^2\cos^2\varphi + \sin^2\varphi}}, \qquad F = (1.13-0.09\varepsilon)(1+0.1(1-\sin^2\varphi)), \qquad \varepsilon = a/c, \quad k = \sqrt{1-\varepsilon^2},$$

$$f = \left(\sin^2\varphi + \varepsilon^2\cos^2\varphi\right)^{1/4}, \qquad B = \left(k^2-\nu\right)E_s + \nu\varepsilon^2 D.$$

E_s – elliptic integral of the second kind, D – elliptic integral of the first kind, $\delta_{II}, \delta_{III}$ - polynomial correction of solution for the full elliptical crack [3].
After substitution of the received stress intensity factors in Williams type solution [6]

$$\begin{cases} \begin{bmatrix} \sigma_{xx} & \sigma_{xy} \\ \sigma_{yx} & \sigma_{yy} \end{bmatrix} = \frac{K_1}{\sqrt{2\pi r}}\begin{bmatrix} f_{1,xx}(\theta) & f_{1,xy}(\theta) \\ f_{1,yx}(\theta) & f_{1,yy}(\theta) \end{bmatrix} - \frac{K_2}{\sqrt{2\pi r}}\begin{bmatrix} f_{2,xx}(\theta) & f_{2,xy}(\theta) \\ f_{2,yx}(\theta) & f_{2,yy}(\theta) \end{bmatrix} + \begin{bmatrix} T & 0 \\ 0 & 0 \end{bmatrix} \\ \sigma_{xz} = -\frac{K_{III}}{\sqrt{2\pi r}}\sin\frac{\theta}{2}; \quad \sigma_{yz} = \frac{K_{III}}{\sqrt{2\pi r}}\cos\frac{\theta}{2}; \quad \sigma_{zz} = \nu(\sigma_{xx}+\sigma_{yy}) \end{cases} \qquad (4)$$

a stress-strain state for all mixed mode cases is determined. The offered solution considers biaxiality, crack orientation angle, form and section position along the curvilinear front for the inclined surface cracks behavior description.

3. Predicting crack growth direction

As follows from the analysis of mixed mode problems [9], all fracture modes are encountered along the crack front when the inclined surface crack is subjected to remote uniform biaxial loading at different intensities. Due to the stress intensity factors changes along the crack front, the crack growth direction angles must also change from point to point along the crack front. This leads to different degrees of non-planar extension along the crack front.

In the present work strain energy density criterion is used to determine the angle of crack propagation (θ^*).The strain energy density criterion was introduced by Sih [7], and it is based on the assumption that a continuum may be presented as an assembly of small elements, each of them containing a unit volume of solid that can store a finite amount of energy at a given instance of time. The energy per unit volume was called the strain energy density function dW/dV.

The SED theory predicts a failure by fracture and/or yielding, and it is based on the following hypotheses:

– location of fracture initiation is assumed to coincide with the maximum or minimum (dW/dV);

– a fracture initiate at the location where (dW/dV) reaches a critical value $(dW/dV)_c$ is a characteristics of the material;

– once a crack is extended after reaching $(dW/dV)_c$, it can be propagated stably. Therefore, the SED can be determined by the following expression

$$(dW/dV)_c = S_c / r_c, \tag{5}$$

where $(dW/dV)_c$ is the area under the true stress and strain curve, while r_c is the distance from the tip to the point where global instability starts.

Thus, a line drawn from each point on the crack front in the normal plane at the angle θ^* with respect to the crack plane indicates the directions in which the strain energy density has its minimal value, which is where

$$\frac{\partial \overline{W}}{\partial \theta} = 0, \quad \frac{\partial^2 \overline{W}}{\partial \theta^2} > 0, \; \overline{W} = dW/dV. \tag{6}$$

For linear elastic material behavior the strain energy density function (dW/dV) can be written as

$$\frac{dW}{dV} = \frac{1}{2}\left(\sigma_{xx}\varepsilon_{xx} + \sigma_{yy}\varepsilon_{yy} + \sigma_{zz}\varepsilon_{zz} + \sigma_{xy}\gamma_{xy} + \sigma_{yz}\gamma_{yz} + \sigma_{zx}\gamma_{zx}\right) =$$
$$= \frac{1}{2}\left[\begin{array}{l} \sigma_{xx}\dfrac{\partial u}{\partial x} + \sigma_{yy}\dfrac{\partial v}{\partial y} + \sigma_{zz}\dfrac{\partial w}{\partial z} + \sigma_{xy}\left(\dfrac{\partial v}{\partial x} + \dfrac{\partial u}{\partial y}\right) + \\ + \sigma_{yz}\left(\dfrac{\partial w}{\partial y} + \dfrac{\partial v}{\partial z}\right) + \sigma_{zx}\left(\dfrac{\partial u}{\partial z} + \dfrac{\partial w}{\partial x}\right) \end{array}\right] \tag{7}$$

where $\sigma_{ij}, \varepsilon_{ij}$ - are stress and strain components, u, v, w - are displacement components [6]. Application of Eqs. (1-4) and (7) and performing the necessary algebra, the expansion of the strain energy density field is resulting for inclined surface semi-elliptical crack subjected to biaxial loading

$$\frac{dW}{dV} = \frac{1}{4G\pi r}\left(a_{11}K_I^2 + a_{12}K_I K_{II} + a_{22}K_{II}^2 + a_{33}K_{III}^2\right) + \frac{1}{2G\sqrt{2\pi r}}\left(b_{11}K_I + b_{22}K_{II}\right) + \frac{T(1-\eta)\sigma}{16G}c_T \tag{8}$$

Full expressions for coefficients in Eq.8 are given in [8]. Substituting Eq. (8) into Eq. (6), the values of θ^* at all points of the crack periphery can be calculated for different combinations of biaxial load, crack orientation angle and surface flaw geometry (Fig.3).

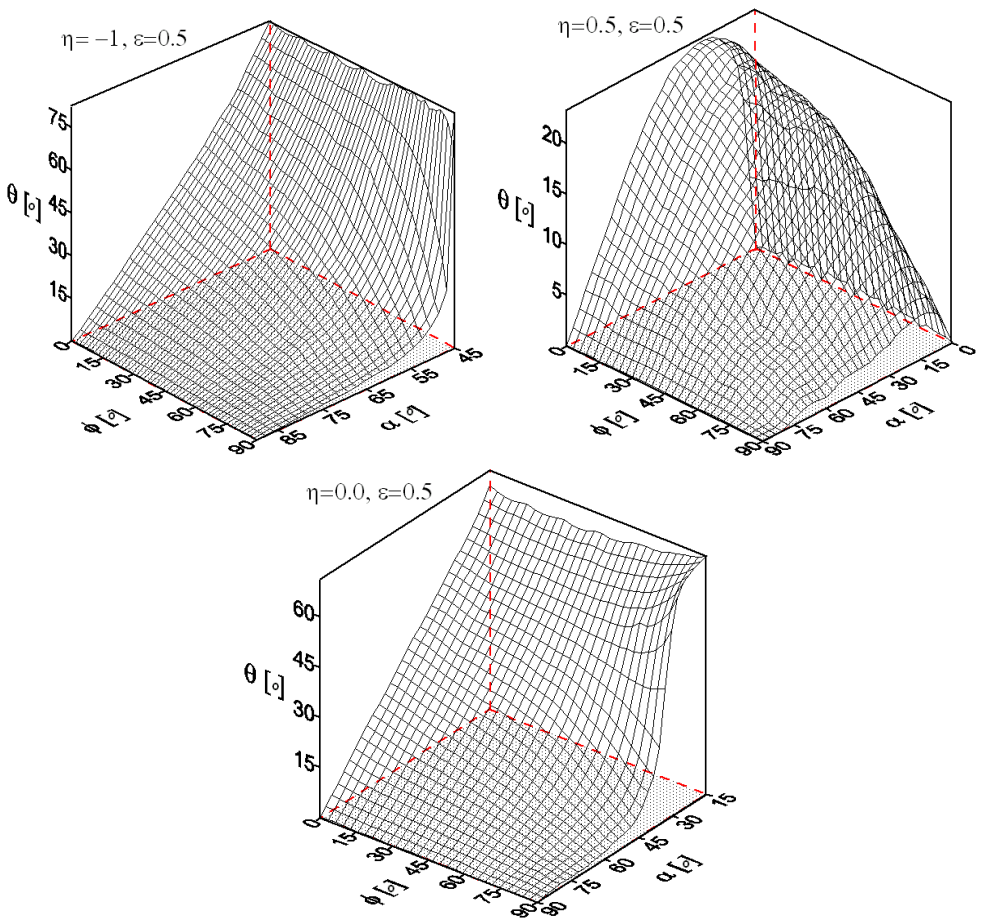

Figure 3. Crack propagation angles along inclined crack fronts

Fig. 3 shows the behavior of the crack growth direction angle θ^* along the surface crack front for dimensionless crack tip distance r/a = 0.01. It shows that the load biaxiality and orientation angle has a principal effect on the crack growth direction angle along the crack front.

4. Mixed mode surface crack growth direction

Precracking under ASTM E740-03 [1] was the first stage of the tests. In a plate center semielliptical saw cut with deepest point 3mm and a/c ratio fixed at 0.3 was made. Precracking has been performed on servo-hydraulic Biss-00-201 plug-n-play test system in three point bend conditions (Fig.4). Crack size 2c=28 millimeters on free surface for all specimens was reached. Specimens from A248 steel with standard mechanical characteristics were executed: yield stress – 225 MPa, ultimate strength– 425MPa, Yang module – 206GPa.

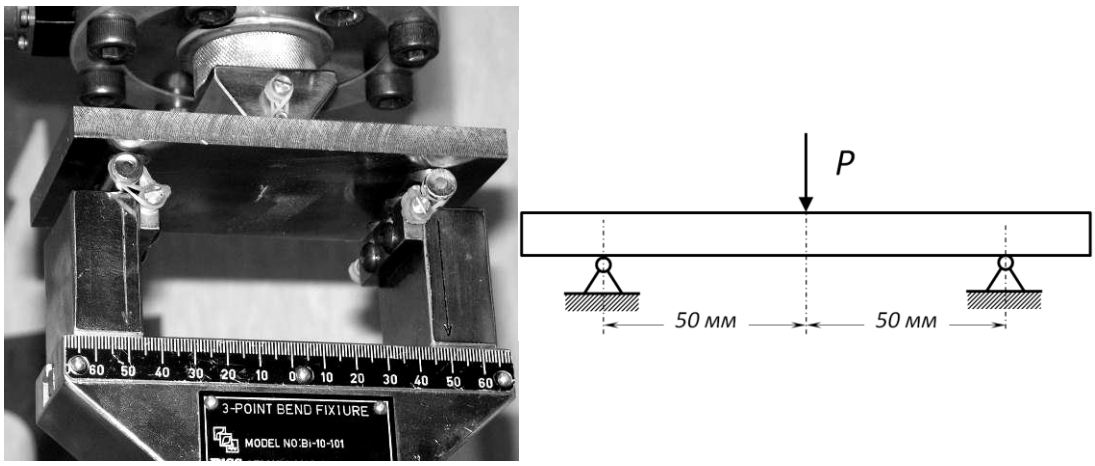

Figure 4. Specimen precracking

Next tests stage was mixed mode surface crack growth direction detection under uniaxial tension and three point bend conditions. Mixed mode has performed initial crack angle change relative to the load axis for uniaxial tension (Fig.5a) and specimen turn relative to test tool set for three point bend case (Fig.5b).

a) b)

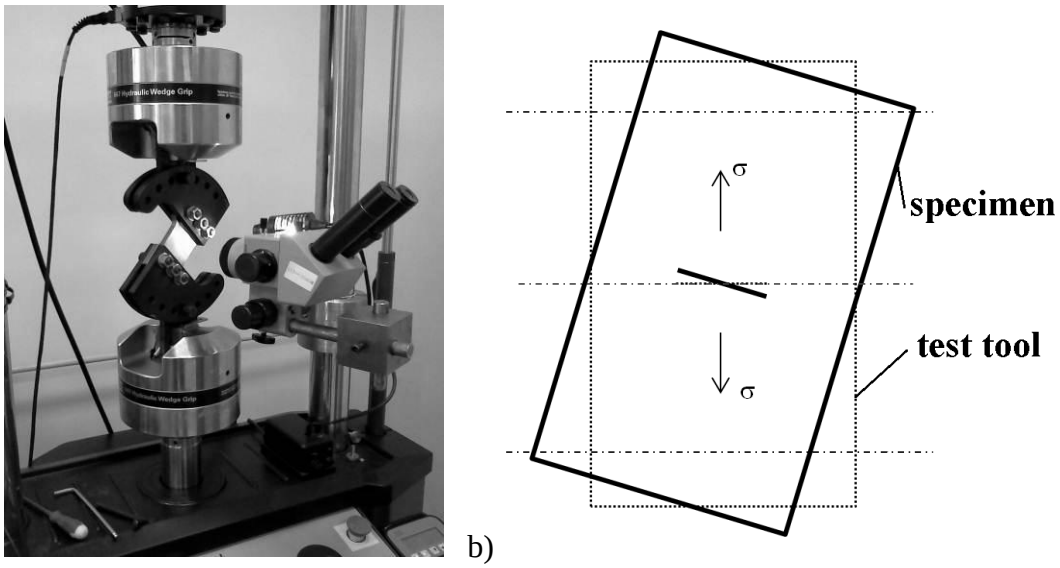

Figure 5. Mixed mode implementation

Uniaxial tension tests are implemented by MTS Landmark servohydraulic system. Crack orientation angle is fixed at 60^0 that is bound to test systems possibilities.

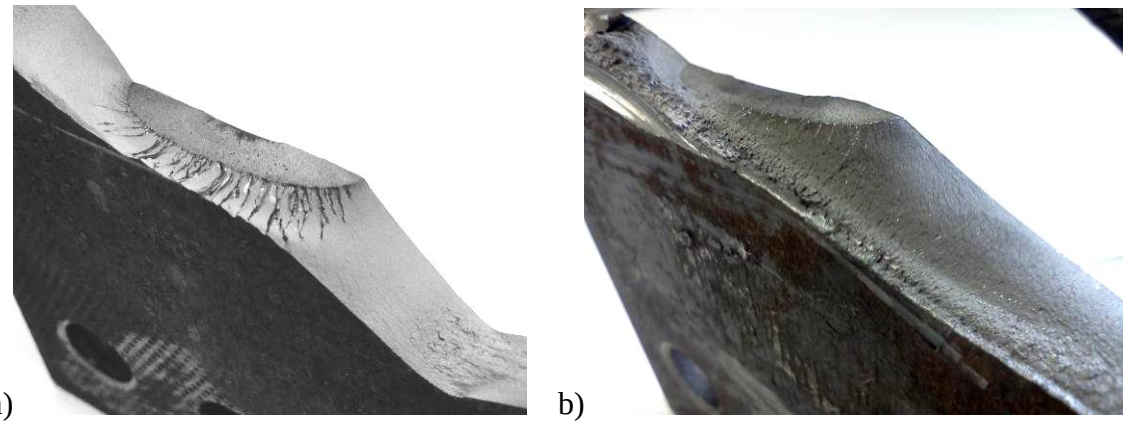

a) b)

Figure 6. Mixed mode fracture surfaces (a – uniaxial tension, b – three point bend)

The test results are fracture surfaces presented in Fig.6. The surfaces analysis specifies that crack growth direction along curvilinear front is variable and depends on front section position. Mode III destruction observed in a deepest crack front point needs consideration. Present circumstance confirms mixed mode transitions along crack front motion.

Crack growth direction in characteristic crack front sections (free surface and deepest point) with design value coincides accurate within 12 percent (Fig.3). Moreover, observed crack propagation angle with calculated values coincided qualitatively.

5. Interpretation method for surface crack growth

Determination of crack resistance characteristics for mode I surface cracks was a purpose of the next test stage. Two propagation stages for pure tension surface flaws ($a/c<1$ and $c>t$) are experimentally established (Fig.7a). First crack growth stage is accompanied by free surface perpendicular propagation and crack size on free surface remains invariable (c – constant). When the crack front reaches opposite surface the second stage takes its place. In this propagation stage the crack was approximated by trapeziform front.

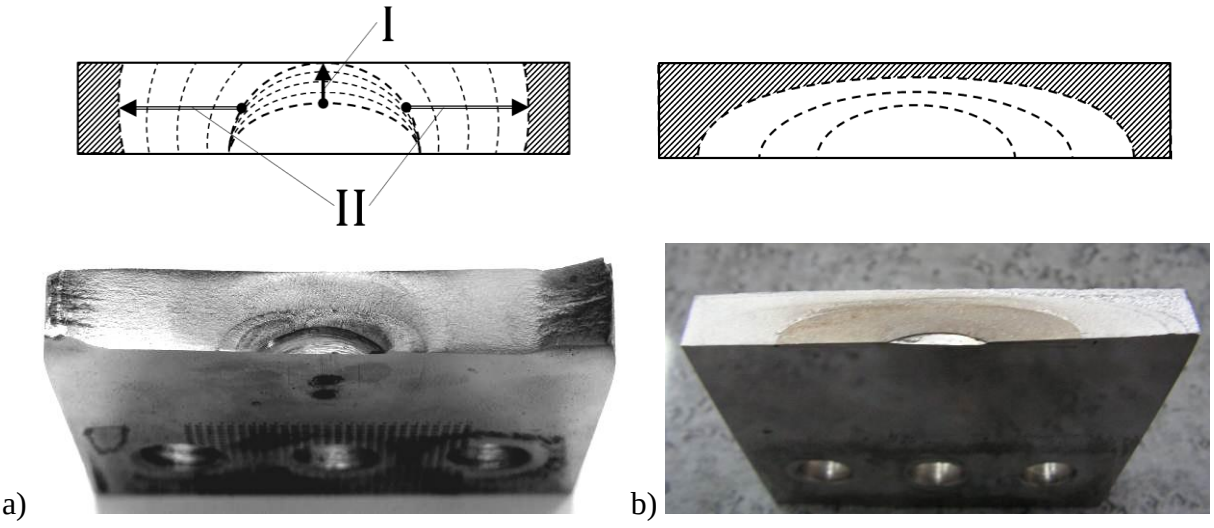

a) b)

Figure 7. Semielliptical cracks
(a – uniaxial tension, b – three point bend)

During the experiment dependence between crack opening displacement and current load cycle was obtained (Fig.8a). Both at pure tension and at three points bend after every 100000 cycles an

overload cycle was applied. Thus, the interrelation between free surface crack size and deepest point was established (Fig.8b).

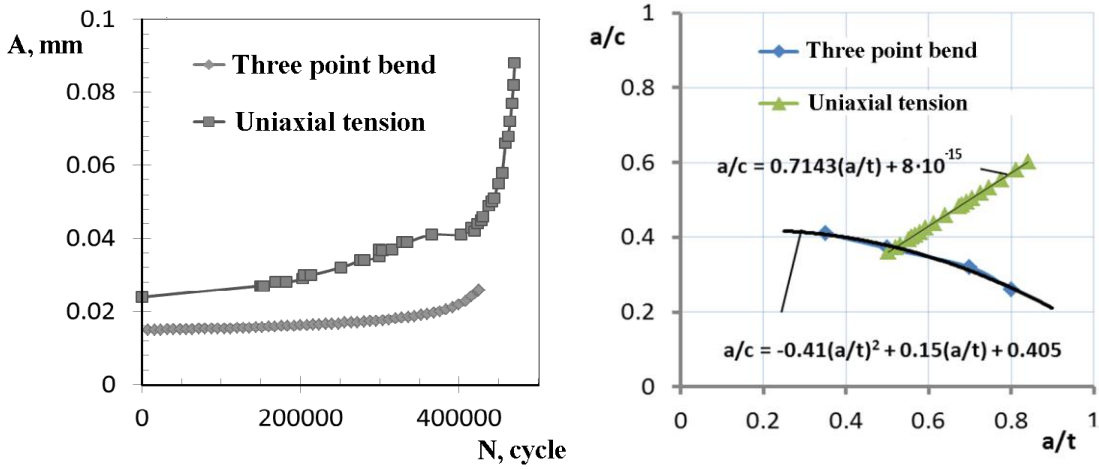

a) b)

Figure 8. Relationships between crack opening displacement and current load cycle (a) and between free surface crack size and deepest point (b)

Experimental equipment makes it possible to fix crack opening displacement depending on load cycle automatically. It allows determining the relationship between crack opening displacement and surface flaw geometry that is necessary to analyze the results. These dependences were received by finite element method. The finite element meshes based on the experimental dependences of the free surface crack size and deepest point for various growth stages were formed (Fig.9).

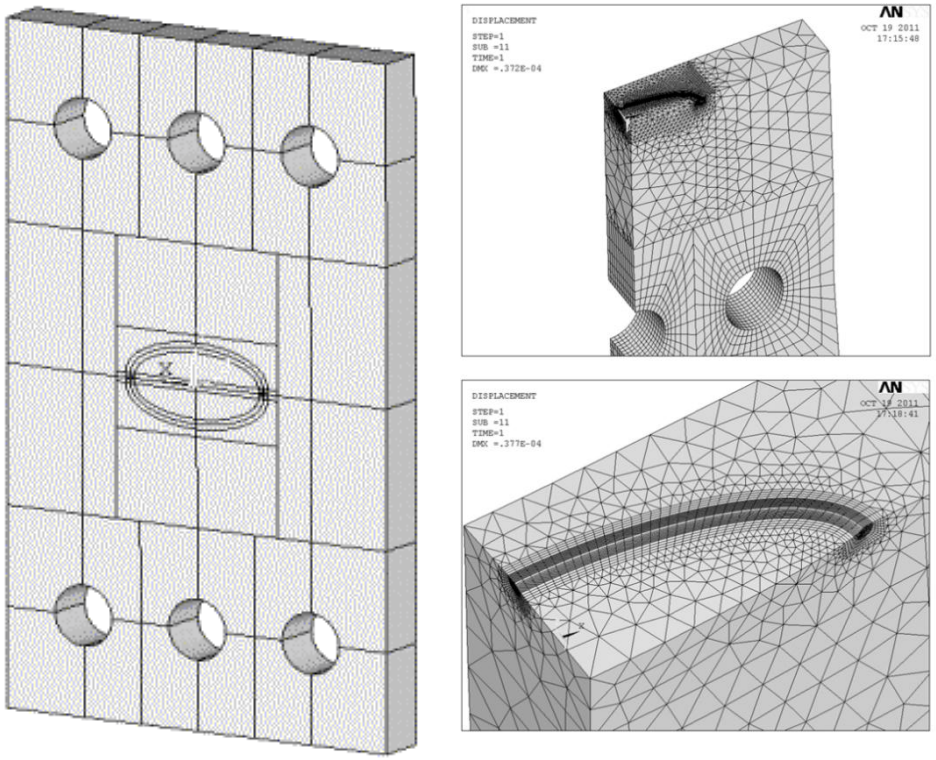

Figure 9. Finite element models of a plate containing inclined semi-elliptical surface crack

Dependences between crack opening displacement and crack front geometry were results of finite element solution (Fig.10).

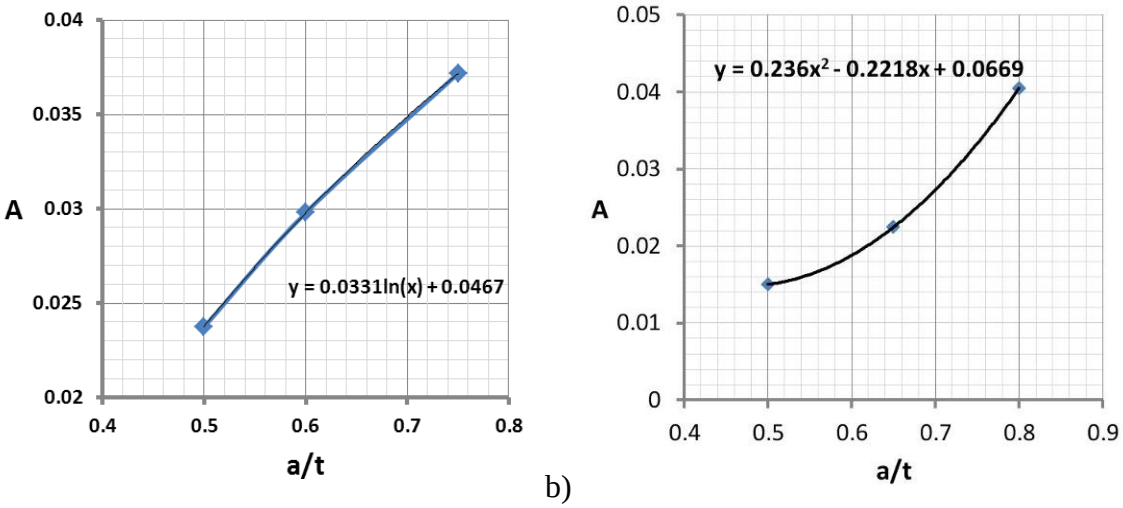

a) b)

Figure 10. Relationship between crack opening displacement and crack front deepest point (a – pure tension, b – three point bend)

Equations (2) and finite element solution allow receiving relationship between stress intensity factors and crack opening displacement (Fig.11).

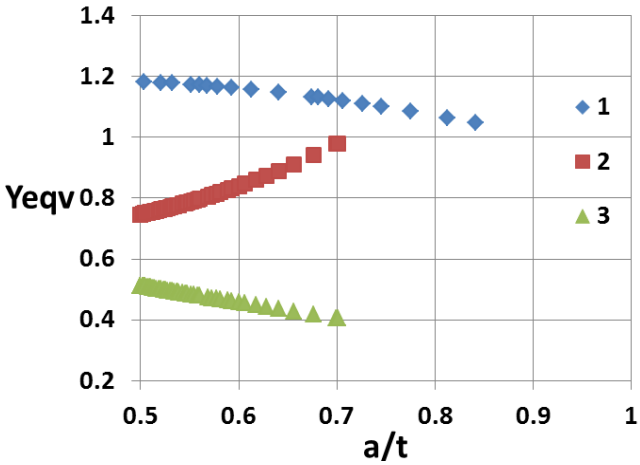

Figure 11. Stress intensity factors distributions

(1 – pure tension, $\varphi = 90^0$; 2 – three point bend, $\varphi = 0^0$; 3 – three point bend, $\varphi = 90^0$)

Experimental data allows graph dependences between maximal along surface crack front stress intensity factor and crack growth rate. For the first stage uniaxial tension case (Fig.7a) maximal stress intensity factor in the crack front deepest point is observed. In three point bend case maximal stress intensity factor is located on the free surface. Received crack extension curves for surface crack growth are presented in Fig.12.

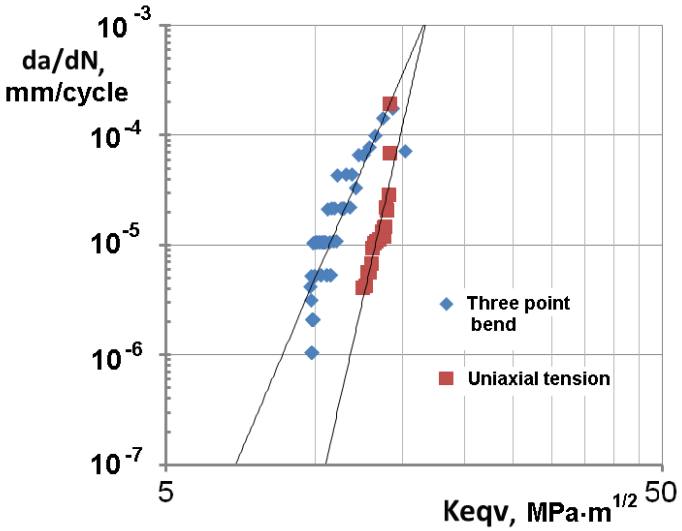

Figure 12. Crack extension curves for uniaxial tension and three point bend conditions

These relationships allow determining crack resistance characteristics in selected crack front sectors. Linear part of the fatigue crack growth rate graph was described by the Paris-Erdogan equation.

$$\frac{da}{dN} = CK_{\max}{}^{m} \tag{9}$$

Table 1 is a result of statistical data processing. From the presented results it follows that surface crack growth rate is bigger in three point bend case. This circumstance allows to draw a conclusion that three point bend is more dangerous load case.

Table 1. Surface cracks resistance characteristics

	Three point bend	Uniaxial tension	
	Free surface, $\varphi = 0^0$	Crack front deepest point Stage I, $\varphi = 90^0$	Trough crack growth C_{eqv}
C	0.115672E-06	0.765931E-05	0.827936E-20
m	1.7958	1.0200	13.4137

Earlier two propagation stages were noted. The first crack growth stage is accompanied by free surface perpendicular propagation, and the crack size on free surface remains invariable. When the crack front reaches the opposite surface the second stage comes. In this propagation stage the crack was approximated by trapeziform front (Fig.13). Crack growth rate was defined in two sections. The first section corresponds to free surface (A). In this plane the crack has a maximal observable size. The second section was in the middle of the plate.

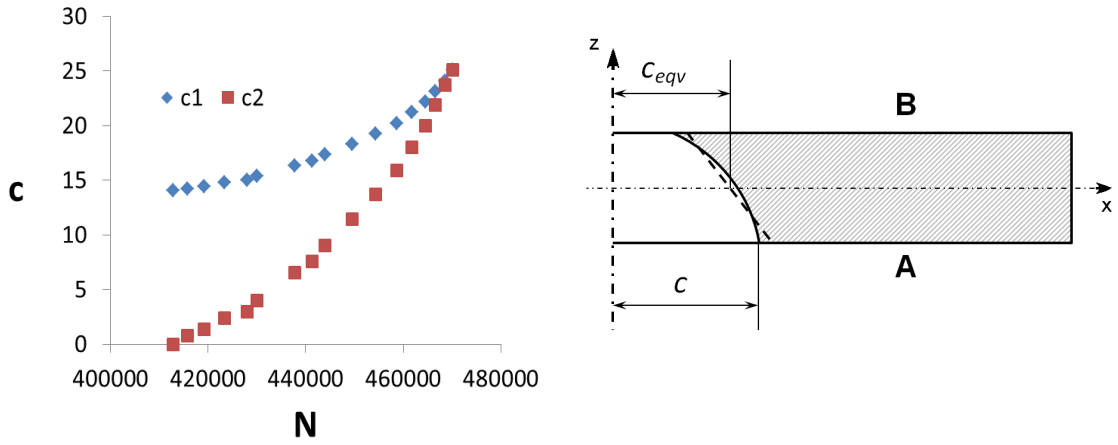

Figure 13. Equivalent crack length

Efficient crack size was determined as:

$$c_{eqv} = \frac{c_A + c_B}{2} \tag{10}$$

Stress intensity factors for trapeziform crack were determined in [5]:

$$K_I = F\sigma\sqrt{\pi c}, \qquad F = \left(1.99 - 0.41\left(\frac{2c}{W}\right) + 18.7\left(\frac{2c}{W}\right)^2 + 53.85\left(\frac{2c}{W}\right)^4\right)\pi^{-1/2} \tag{11}$$

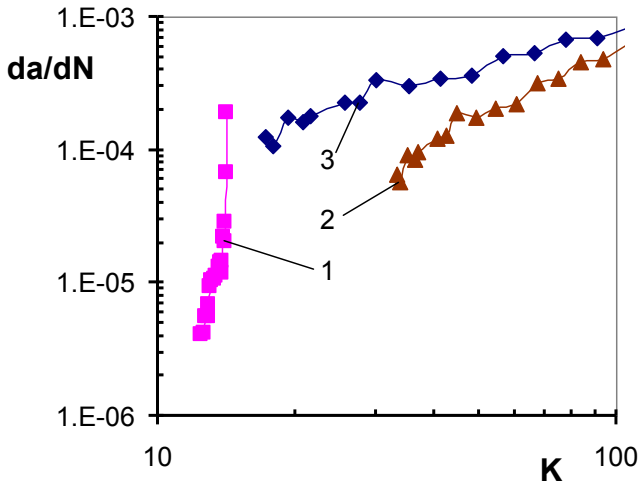

Figure 14. Surface crack growth rate in uniaxial tension case
(1 – stage I; 2 – stage II, free surface; 3 - stage II, middle section)

Crack growth rate depending on stress intensity factors in uniaxial tension case are present in Fig.14. The curve 1 corresponds to the first propagation stage. Curves 1 and 3 allow presenting a crack growth rate graph as a spline. Paris-Edrogan equation constants for equivalent crack size are included in Tab.1. Curves 1 and 3 represent consecutive growth stages. When the crack front reaches opposite surface it corresponds to inflection point. From the crack growth stages comparison it is possible to affirm that the first stage corresponds to higher crack growth rate.

Conclusion

The mixed mode behavior of crack growth direction angle along semi-elliptical crack front for different combinations of biaxial loading, inclination crack angle and surface flaw geometry were considered. Crack resistance characteristics under uniaxial tension and three point bend conditions for surface crack were obtained. Two propagation stages of pure tension surface cracks accompanied by the crack growth rate change were established.

Acknowledgments

The authors gratefully acknowledge the financial support of the Ministry of Education and Science of the Russian Federation under the state contract №16.516.11.6045.

Reference

1. Standard for Fracture Testing with Surface-Crack Tension Specimen / E 740-03, ASTM International, West Conshohocken, 2003, 9p.
2. ASTM E647 - 11e1 Standard Test Method for Measurement of Fatigue Crack Growth Rates
3. He, M.Y., Hutchinson, J.W., 2000. Surface crack subject to mixed mode loading. Engineering Fracture Mechanics 65, 1–14.
4. Kassir, M.K., Sih, G.C., 1966. Three-dimensional stress distribution around an elliptical crack under arbitrary loadings. Journal of Applied Mechanics 33, 141–152.
5. Murakami, Y. (Ed.), 1990. Stress Intensity Factors Handbook. Pergamon Press.
6. Eftis J., Subramonian N. The inclined crack under biaxial load //Engineering Fracture Mechanics.- 1978. - 10. - P. 43-67.
7. Shih, C.F., 1974. Small-scale yielding analysis of mixed plane strain crack problem. In: Fracture Analysis, ASTM STP 560. ASTM, Philadelphia, PA, pp. 187–210.
8. 3. Shlyannikov V.N., Kislova S.Yu., Tumanov A.V. Inclined semi-elliptical crack for predicting crack growth direction based on apparent stress intensity factors // Theoretical and Applied Fracture Mechanics, 2010 vol..53, pp.185-193.
9. 7. Shlyannikov V.N., Tumanov A.V. An inclined surface crack subject to biaxial loading // International journal of Solids and Structures, 2011, vol.48, pp.1778-1790